SENSITIVITY OF SEABED MORPHOLOGY TO HYDRODYNAMIC AND SEDIMENT TRANSPORT PARAMETERS IN TIDAL SYSTEMS

MUSA, M. A.[1] – AHMAD, M. F.[1*] – GOH, S. E. G.[1]

[1] *Faculty of Ocean Engineering Technology, Universiti Malaysia Terengganu, Terengganu, Malaysia.*

**Corresponding author*
e-mail: fadhli[at]umt.edu.my

(Received 26th May 2025; revised 05th September 2025; accepted 17th September 2025)

Abstract. Sediment transport and seabed evolution are key processes influencing the morphology and stability of coastal and estuarine systems. This study uses a one-dimensional (1D) coupled hydrodynamic–sediment transport model to simulate shallow water flow and sediment dynamics in the Kuala Terengganu region. The model integrates the Saint-Venant shallow water equations with the Exner equation for bed evolution and the advection–diffusion equation for suspended sediment concentration. Numerical implementation using the finite volume method ensures mass conservation and numerical stability, allowing accurate representation of flow–sediment feedback. The objectives are: (1) to simulate the temporal evolution of seabed morphology and quantify long-term bed elevation changes; (2) to evaluate the effects of hydrodynamic parameters, particularly tidal range and bed friction coefficient, on sediment entrainment, deposition, and erosion; and (3) to assess the influence of sediment transport parameters, especially the Grass coefficient, on seabed stability and erosion–deposition dynamics. Results show a non-linear decline in bed elevation with a 38% reduction over three years, indicating rapid early sediment mobility followed by stabilization. Increasing tidal range enhances sediment removal, while friction and Grass coefficients govern the transition between erosion and deposition. The findings provide insights for predicting coastal morphological change and improving sediment management.
Keywords: *sediment transport, seabed evolution, hydrodynamic modeling, coastal morphology*

Introduction

Sediment transport and seabed evolution are fundamental processes governing the stability and morphology of coastal and estuarine environments (Wu et al., 2025; Amoudry and Souza, 2011). The dynamic interaction between hydrodynamics and sediment motion determines not only the geomorphic evolution of riverine and coastal systems but also affects navigation channels, coastal habitats, and sediment budgets, and more broadly in coastal morphodynamics (Rasyif et al., 2017). Accurate prediction of these processes is therefore critical for effective coastal zone management, infrastructure design, and ecosystem preservation. However, understanding the coupled behavior of fluid flow and sediment transport remains a complex challenge due to the nonlinear feedbacks between flow hydraulics, bed roughness, and sediment mobility (Cheng et al., 2007). In recent years, numerical modeling has become a key tool for investigating sediment transport dynamics under various hydrodynamic conditions (Pareta, 2024). One-dimensional (1D) models, in particular, provide an efficient yet physically robust framework to simulate shallow water flow and sediment transport over extended temporal and spatial scales (Hou et al., 2020). These models capture the essential physics governing flow continuity, momentum, and sediment exchange, offering valuable insights into morphological evolution without the computational demand of higher-dimensional simulations (Salheddine et al., 2020).

The Saint-Venant shallow water equations (SWEs), coupled with the Exner equation for bed evolution and the advection–diffusion equation for suspended sediment transport, form the theoretical basis of many sediment transport studies (Jelti and Serghini, 2023). By integrating these governing equations within a finite volume numerical framework, it is possible to achieve mass conservation and numerical stability while resolving the dynamic feedbacks between flow and sediment processes. Such an approach is particularly useful for analyzing how key parameters, such as tidal range, bed friction, and the Grass coefficient, affect sediment entrainment, deposition, and long-term morphological change. In this study, a 1D coupled hydrodynamic–sediment transport model is developed and applied to a representative coastal environment in the Kuala Terengganu region. The model serves as a numerical laboratory to explore the influence of key physical and empirical parameters on seabed evolution under tidal forcing. The specific objectives of this research are to: (1) Simulate the temporal evolution of seabed morphology using a coupled hydrodynamic–sediment transport framework to quantify long-term trends in bed elevation. (2) Examine the influence of hydrodynamic parameters, particularly tidal range and bed friction coefficient, on sediment entrainment, deposition, and net bed change. (3) Evaluate the role of sediment transport parameters, including the Grass coefficient, in controlling erosion–deposition dynamics and overall seabed stability. Through these objectives, the study aims to enhance understanding of sediment transport mechanisms in shallow tidal environments and provide a basis for improving predictive modeling of coastal morphological change.

Materials and Methods

This study employs a one-dimensional (1D) coupled hydrodynamic and sediment transport model to investigate shallow water flow and the corresponding sediment dynamics. The methodology integrates governing equations for fluid motion and sediment processes, a numerical solution scheme, and carefully selected input parameters to ensure realistic and replicable simulations. Key components include the Saint-Venant shallow water equations coupled with the Exner equation for bed evolution and an advection-diffusion equation for suspended sediment transport. A finite volume method is used to discretize and solve the coupled equations, ensuring both numerical stability and mass conservation. Initial parameter values were selected to reflect representative coastal and hydraulic conditions in the Kuala Terengganu region, while sensitivity analyses explored a range of parameter values to account for uncertainties in environmental and hydraulic variability. Figures summarize the simulation setup, including initial bed configuration, parameter ranges, and values employed for long-term sediment transport analysis.

Hydrodynamic and the transport of sediment

A one-dimensional (1D) coupled hydrodynamic–sediment transport model is used to simulate shallow water flow and its associated sediment dynamics. The model integrates the Saint-Venant shallow water equations (SWEs), comprising the continuity and momentum equations, with the Exner equation for bed evolution and an advection–diffusion equation for suspended sediment transport. The conservation of mass for the water column is described by the continuity equation (Díaz et al., 2008):

$$\frac{dh}{dt}+\frac{d(hu)}{dy}=0 \qquad \text{Eq. (1)}$$

Where, u is the velocity average over height (m/s), h is the elevation of water (m), t is simulation duration (s), and y is horizontal distance (m). The water flow momentum as follows (Simpson and Castelltort, 2006):

$$\frac{d(hu)}{dt}+\frac{d}{dy}(hu^2+\frac{1}{2}gh^2)=-gh\frac{dz_b}{dy}-C_f v|v| \qquad \text{Eq. (2)}$$

Where, g as gravity (m/s^2), z_b as elevation of sea floor (m), and C_f as coefficient of friction (s^2/m). Sediment transport is modelled using two primary equations. First, the bed evolution due to sediment transport is governed by the Exner equation (Paola and Voller, 2005):

$$\frac{dz_b}{dt}+\frac{1}{1-\lambda}\frac{dQ_s}{dy}=0 \qquad \text{Eq. (3)}$$

Where, that λ is the porosity of the sea floor (no dimension), and Q_s is the volumetric sediment flow in volume rate per unit wide (m^2/s). The particle in suspension concentration, I (kg/m^3), governed by advection-diffusion equation (Huai et al., 2020):

$$\frac{d(hI)}{dt}+\frac{d(hIv)}{dy}=\frac{d}{dy}(D_s\frac{dI}{dy})+S \qquad \text{Eq. (4)}$$

Where, D_s is diffusivity of particle concentration (m^2/s), and S as addition or removal term (kg/m²/s) correspondingly refer to entrainment and deposition. The volumetric sediment flow in volume rate per unit wide Q_s (m^2/s) is represented in (Grass, 1981):

$$Q_s=A_g|v|^m v \qquad \text{Eq. (5)}$$

Where, A_g known as the Grass coefficient (s^2/m), m is constant could be ranged 3 and 5, and $|v|v$ refers to direction and nonlinearity.

Numerical method

The coupled equations are discretized and numerically solved using the finite volume method, ensuring both mass conservation and numerical stability. This approach enables dynamic interactions between flow hydraulics and sediment transport processes, which are essential for accurately capturing morphological evolution in riverine and coastal systems.

Default simulation input

In the sediment transport simulation, as in *Figure 1*, several default parameters were applied with their values expressed in logarithmic form for comparative purposes. The grass coefficient (Ag) was assigned a log value of –3, corresponding to an actual value

of 0.001 s²/m that a lower value than this could be reflecting coarse or gravel. The tidal range was given a log value of 0.3010, equivalent to 2.0 m, representing the vertical difference between high and low tides. Gravity was set at a log value of 0.9917, corresponding to 9.8 m/s², which reflects Earth's gravitational acceleration. The simulation time was defined with a log value of 6.1918, equivalent to approximately 1.55×10^6 seconds. Friction (Cf) had a log value of –2.699, translating to an actual value of about 0.002, indicating very low resistance consistent with smooth bed conditions. The medium length parameter was assigned a log value of 4, corresponding to 10,000 m, while the water height was set at a log value of 1.3010, equivalent to 20 m. These parameters collectively represent the baseline conditions for simulating wave–sediment interactions in the computational model.

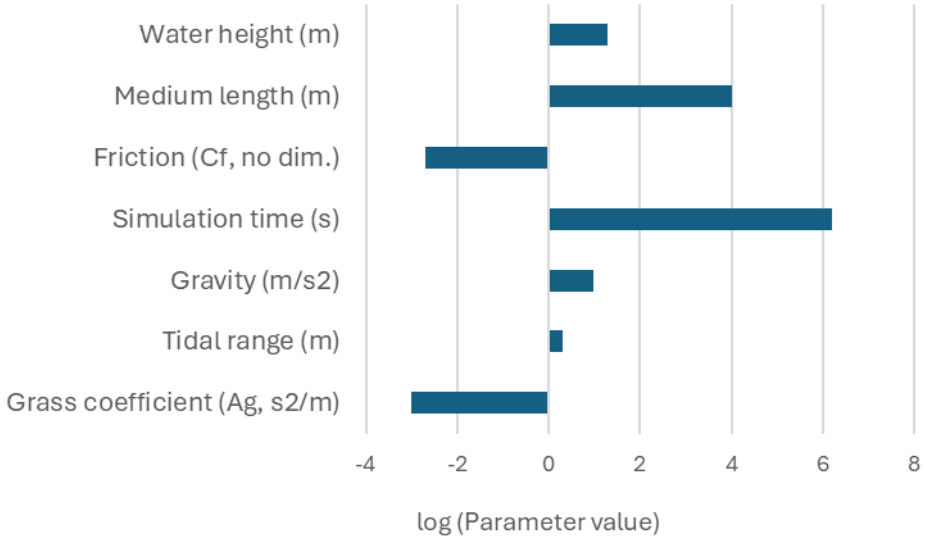

Figure 1. *Default simulation parameters, assigned values, and units for sediment transport. Note: the value is log to allow relative comparison among parameters. The negative value indicates it's before log value is less than unity. Also, no dim refers to dimensionless.*

Bed elevation before simulation begins

Figure 2 is the initial condition of the simulated medium shows a predominantly flat seabed extending from 0 to 10 km, with the bed elevation remaining at 0 m across most of the domain. A localized elevation feature is present between approximately 3.1 km and 4.9 km, forming a smooth mound that rises gradually to a maximum height of about 0.98 m near 3.9–4.1 km before symmetrically sloping back down to the flat bed level. This seabed configuration serves as the baseline topography prior to the onset of tidal wave forcing, providing a controlled setup to examine how wave propagation interacts with both flat and elevated sections of the sea floor and to capture the resulting hydrodynamic and sediment transport responses.

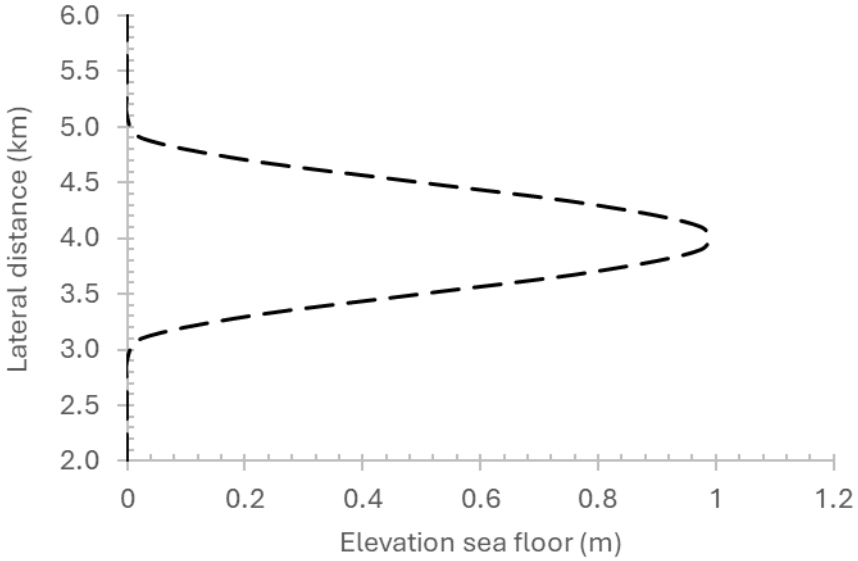

Figure 2. *Side view of the simulated medium showing the elevation sea floor, with the tidal wave propagating from 0 to 10 km.*

Minimum and maximum value range on parameters

The simulation parameters investigated were expressed in logarithmic values to enable relative comparison across different scales, *Figure 3*. The grass coefficient (Ag) ranged from −3.301 to −1.155 in log10, corresponding to antilog values between 0.0005 and 0.07 s^2/m, capturing nearly two orders of magnitude in sea floor resistance, all below unity due to the negative logs. The tidal range spanned 0.255 to 0.431 in log10, or 1.8 to 2.7 m in real values, reflecting a moderate variation within realistic tidal conditions. Simulation time extended from 6.891 to 7.970 in log10, equivalent to 7.8×10^6 to 9.3×10^7 seconds (roughly 90 days to 3 years), thus encompassing both seasonal and multi-year dynamics. Finally, the friction coefficient (Cf) varied widely from −6 to 0 in log10, translating to 10^{-6} to 1, a range spanning six orders of magnitude from extremely smooth to very rough flow conditions. Altogether, the log-based formulation highlights both fine-scale variability and broad parameter coverage, with negative log values marking quantities smaller than unity and positive values denoting larger magnitudes.

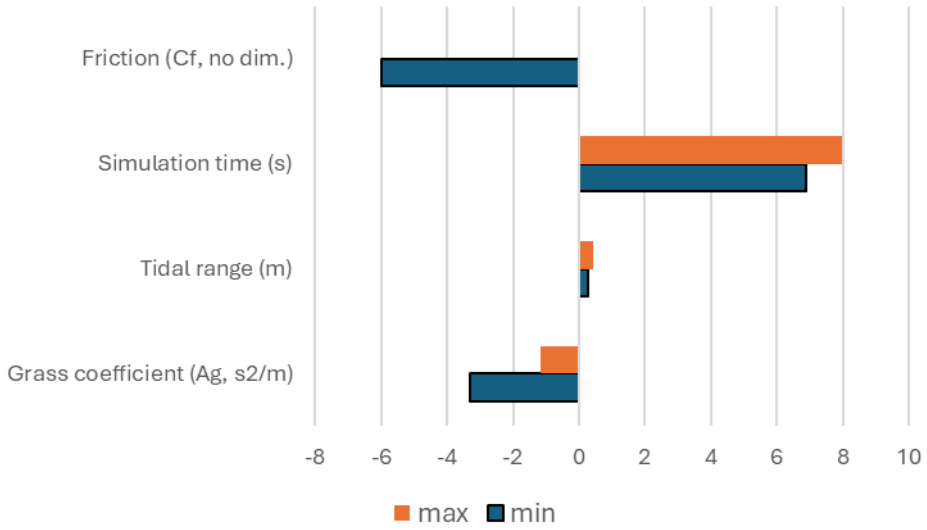

Figure 3. *Minimum and maximum values used in the computer simulation.*
Note: the value is log to allow relative comparison among parameters. The negative value indicates it's before log value is less than unity. Also, no dim refers to dimensionless.

Results and Discussion

Temporal evolution effect

The temporal evolution of sea floor bed height indicates a progressive reduction in elevation due to sediment transport (*Figure 4*). At the initial condition (t=0 yr), the bed height measured 0.9755 m. Within the first 0.25 years, a noticeable decline was observed, with the elevation decreasing to 0.9053 m, corresponding to a 7.2% reduction. By 0.5 years, the bed height further decreased to 0.8545 m, indicating continuous lowering of the bed surface. After one year, the bed elevation reduced to 0.7767 m, marking a net decline of approximately 20% relative to the initial condition. Long-term observations revealed further bed degradation: at 2 years the bed height reached 0.6717 m, and by 3 years it stabilized around 0.6026 m. This represents a total decline of 38.2% from the starting elevation. Overall, the results demonstrate a non-linear but consistent downward trend in bed height, with the most rapid changes occurring during the first year, followed by slower rates of reduction thereafter.

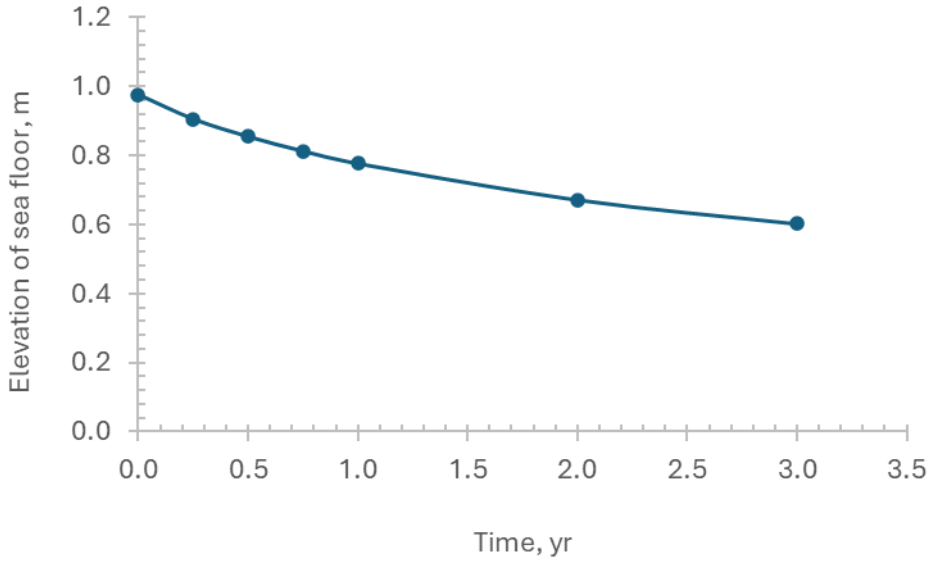

Figure 4. *From zero to 3 years computer simulated results on the elevation of sea floor.*

The observed decrease in sea floor bed elevation reflects active sediment transport processes that progressively remove material from the surface. The sharp decline during the first year suggests high initial mobility of unconsolidated sediments, likely driven by energetic hydrodynamic forcing (e.g., tidal currents). This rapid phase of adjustment is characteristic of systems where sediment supply and bed stability are initially out of balance. Beyond the first year, the rate of bed lowering decreased, as indicated by the smaller changes between years 2 and 3. This attenuation suggests that the system may be approaching a new equilibrium state. As finer sediments are winnowed away, the residual bed material may consist of coarser fractions or consolidated layers that are more resistant to further erosion. Such behavior aligns with existing models of bed armoring, where transport rates diminish as the easily mobilized fraction is depleted. These findings have important implications for coastal and marine geomorphology. Continuous reduction in bed elevation can influence habitat availability, seabed roughness, and hydrodynamic feedbacks (Sun et al., 2025; Yildiz et al., 2025). Moreover, the results highlight the importance of temporal monitoring, as short-term observations may overestimate long-term transport rates (Fincham and Barry, 2025). The three-year record suggests that while sediment removal is initially intense, the system tends toward stabilization over longer timescales.

Effect of tidal range

The relationship between tidal range and sea floor elevation (bed height) was analyzed using the observation in *Figure 5*. The initial bed height at a tidal range of 2.0 m was recorded as 0.8545 m. Bed height decreased progressively with increasing tidal range beyond this point, reaching 0.7244 m at a tidal range of 2.7 m. Conversely, lower tidal ranges (1.8–1.9 m) corresponded to slightly elevated bed heights of 0.883 m and 0.869 m, respectively. Overall, a negative correlation was observed between tidal range and bed height. Larger tidal ranges corresponded to enhanced sediment removal and a net reduction in bed elevation. *Figure 5* clearly illustrates this trend, showing a nearly linear decline in bed height as tidal range increases from 1.8 m to 2.7 m.

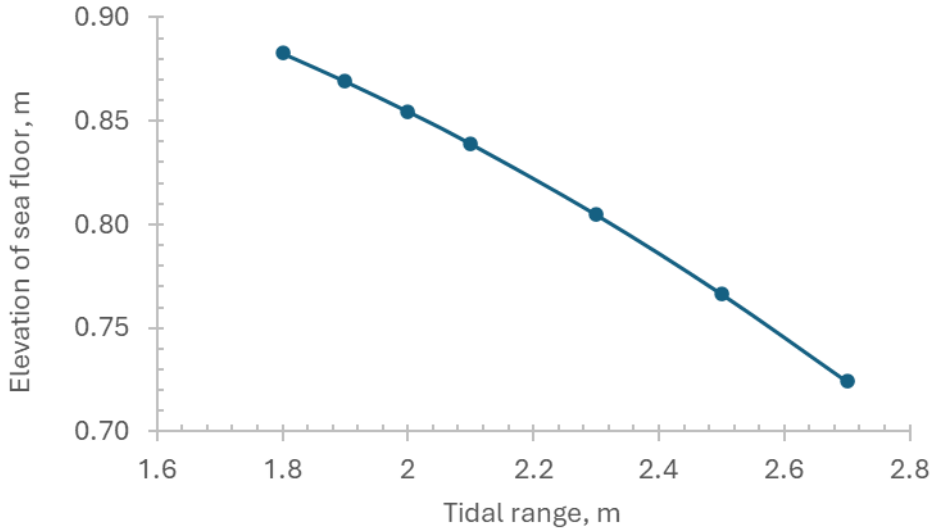

Figure 5. *From 1.8 to 2.7 tidal range computer simulated result on the elevation of sea floor.*

The observed decline in bed elevation with increasing tidal range highlights the direct role of tidal energy in sediment transport processes. Higher tidal ranges are associated with stronger tidal currents and greater bed shear stress, which promote sediment entrainment and export from the bed surface. As a result, sediment loss exceeded deposition under stronger tidal forcing, leading to a measurable reduction in seabed height. At lower tidal ranges (1.8–1.9 m), the relatively reduced hydrodynamic energy permitted limited sediment resuspension, allowing bed levels to remain higher. Around the 2.0 m tidal range, the system may represent a transitional threshold, beyond which the balance tips toward net erosion rather than deposition. This relationship is consistent with previous studies of estuarine and coastal systems, where tidal amplification often drives enhanced erosion and scouring of seabed sediments (Jiang et al., 2020). The linear decline observed trend suggests that tidal range exerts a dominant control on bed height, with other factors kept constant during the study period (Khojasteh et al., 2021). However, in natural systems, interactions with wave forcing, sediment supply, and biological stabilization (e.g., benthic organisms, vegetation) could modulate this relationship. The implications are significant for predicting morphological change in tidally influenced environments. Increased tidal range, whether due to natural variability or anthropogenic drivers such as sea-level rise and channel modifications, may accelerate seabed lowering and alter sediment budgets. Understanding these dynamics is therefore critical for coastal management and sediment transport modeling (Li et al., 2023).

Friction factor on sea floor elevation

The relationship between seabed elevation and the friction factor (Cf) was evaluated across a wide range of Cf values (10^{-6}–1). *Figure 6* summarizes the changes in bed height relative to the initial condition (0.85454 m). At very low friction factors ($Cf \leq 10^{-5}$), the bed elevation showed negligible changes, with values remaining around 0.855 m. A noticeable reduction in bed height occurred when Cf increased to 10^{-4} and 10^{-3}, where elevations decreased to 0.85485 m and 0.85406 m, respectively, suggesting

enhanced sediment mobilization under these conditions. Interestingly, at Cf=0.002, the bed height was nearly identical to the initial condition, suggesting a threshold where erosional and depositional processes balanced. Beyond this point, a sharp increase in bed elevation was observed. At Cf=0.01, the bed height rose significantly to 0.87445 m, indicating deposition. This trend continued with further increases in Cf, reaching 0.95321 m at Cf=0.1 and 0.97288 m at Cf=1. Overall, the results demonstrate a nonlinear relationship between seabed elevation and friction factor: an initial stability at low Cf, a reduction phase at intermediate Cf (10^{-4}–10^{-3}), followed by substantial elevation gain at higher Cf values (≥0.01).

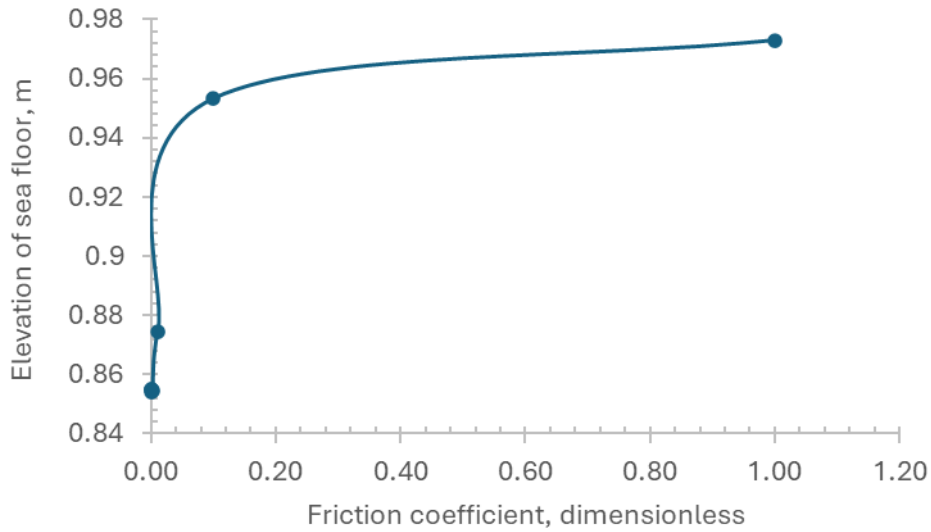

Figure 6. *From 0.000001 to 1 friction coefficient computer simulated result on the elevation of sea floor.*

The results highlight the complex interplay between hydrodynamic stress and sediment transport processes in shaping seabed morphology. At low friction factors (Cf≤10^{-5}), bed elevation changes were minimal, reflecting insufficient bed shear stress to mobilize sediment. Sediment remained largely stable under these conditions, consistent with expectations for low-energy environments. In contrast, the decrease in seabed elevation observed at Cf=10^{-4}–10^{-3} indicates that moderate frictional stresses exceeded the threshold for sediment entrainment. This led to net erosion of the seabed and lowering of the bed profile. Such conditions are typically associated with transitional flow regimes where shear stress enhances sediment transport capacity, but deposition does not yet dominate. The near-restoration of the initial bed height at Cf=0.002 suggests a balance between erosion and deposition, representing a critical threshold of hydrodynamic forcing. Beyond this threshold, as Cf increased above 0.01, the system shifted towards significant deposition. The sharp rise in bed elevation indicates that high friction factors promoted turbulence and suspended load transport, but ultimately enhanced sediment settling and accumulation on the seabed (Dong et al., 2023). This nonlinear pattern has implications for sedimentary dynamics in coastal and shelf environments. It suggests that small increases in hydrodynamic forcing can drive erosion at intermediate regimes, while very high forcing may instead favor deposition due to increased supply and transport of sediment. The findings also point to the importance of accurately parameterizing bed friction in numerical models of sediment

transport, as small changes in Cf can produce markedly different seabed responses (Li et al., 2025).

Grass coefficient on sea floor elevation

The results of the numerical analysis demonstrate a clear relationship between the grass coefficient (A_g) and the evolution of the seabed elevation, as in *Figure 7*. The initial bed height was recorded at 0.8545 m when A_g was 0.001, and subsequent variations in Ag produced progressive reductions in bed elevation. At the lowest coefficient (A_g=0.0005), the bed height was slightly elevated to 0.9053 m, suggesting minimal resistance to sediment mobilization under this condition. However, as A_g increased to 0.0007, the bed height declined to 0.8836 m, marking the onset of sediment transport and redistribution processes. A pronounced decline in seabed elevation was observed with further increments in A_g. At A_g=0.003, the bed height dropped significantly to 0.7180 m, reflecting enhanced scouring and sediment entrainment. This trend continued, with the seabed elevation reducing to 0.5120 m at A_g=0.01 and further to 0.2639 m at A_g=0.04. The lowest seabed height of 0.1530 m was recorded at the maximum A_g tested (0.07), indicating that higher grass coefficients intensify the capacity of flow to erode and transport sediment particles away from the seabed surface.

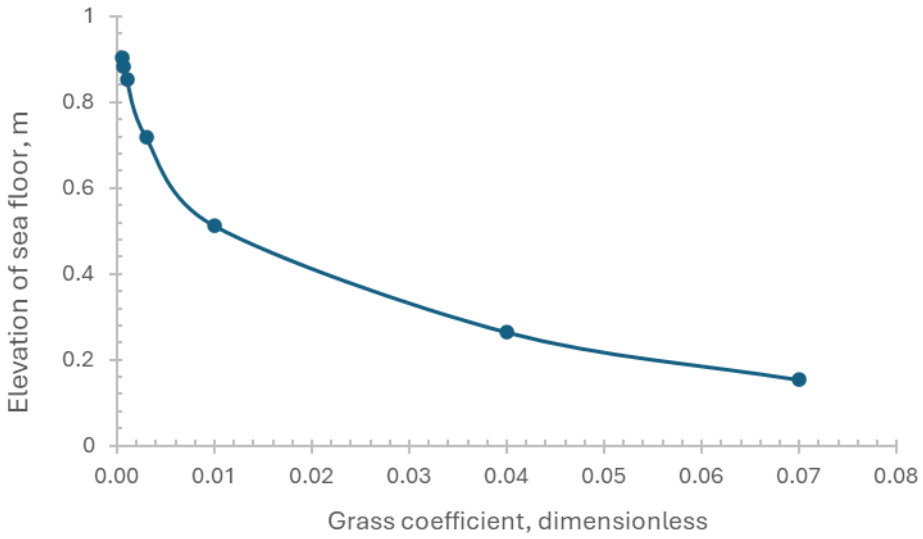

Figure 7. *Grass coefficient effect on elevation of sea floor.*

These results suggest that the grass coefficient plays a critical role in modulating sediment transport dynamics on the sea floor. Lower values of Ag were associated with near-stable bed conditions, while higher values led to significant bed degradation. This behavior can be attributed to the fact that increasing Ag enhances bed roughness, which intensifies turbulence and shear stresses at the sediment-water interface (Penna et al., 2020). Consequently, larger volumes of sediment are entrained and transported, lowering the seabed elevation. From a geomorphological perspective, the observed pattern aligns with classical sediment transport theory, which predicts that increasing flow resistance and turbulence enhances bed shear stresses and accelerates seabed scouring. The rapid decline in bed height at intermediate to high Ag values (0.003–0.07) highlights a nonlinear response, where sediment removal accelerates once a threshold of

roughness is surpassed. This finding has implications for understanding seabed stability in vegetated or roughened marine environments, where the presence of benthic vegetation or roughness elements could markedly influence sediment fluxes and morphological evolution (Papanicolaou et al., 2001).

Conclusion

The simulation results demonstrated that seabed elevation responds non-linearly to variations in hydrodynamic and sediment transport parameters. Temporal analysis revealed a progressive reduction in bed height of up to 38% over three years, with the most rapid degradation occurring during the first year. This initial phase reflects high sediment mobility and energetic forcing, followed by a gradual stabilization period as the bed approached equilibrium. The tidal range analysis indicated a clear negative correlation between tidal amplitude and bed elevation, higher tidal ranges produced stronger currents and enhanced sediment removal, leading to net seabed lowering. The influence of the friction coefficient (Cf) exhibited a complex, non-monotonic relationship with bed elevation. Moderate Cf values (10^{-4}–10^{-3}) promoted erosion through increased shear stress, while higher values (≥ 0.01) led to deposition and seabed buildup, suggesting a threshold between erosional and depositional regimes. Similarly, variations in the Grass coefficient (Ag) strongly affected seabed morphology: higher Ag values intensified turbulence and sediment entrainment, resulting in pronounced seabed degradation. Collectively, the findings highlight the sensitivity of seabed evolution to hydrodynamic forcing, bed friction, and sediment transport parameters. The coupled modeling approach proved effective in capturing the temporal and spatial dynamics of sediment redistribution and morphological change. These results contribute to a better understanding of sediment transport mechanisms in tidally influenced coastal systems and provide a robust framework for predicting seabed response to natural and anthropogenic perturbations. Future work may extend the model to two-or three-dimensional configurations, incorporate wave effects, and validate the simulations against field or laboratory observations to further enhance predictive capability.

Acknowledgement

This research was not funded by any grant. This research was conducted by the student undergraduate study from Bachelor Applied Science Technology Maritime, Faculty Ocean Engineering Technology, University Malaysia Terengganu.

Conflict of interest

The authors confirm that there is no conflict of interest involved with any parties in this research study.

REFERENCES

[1] Amoudry, L.O., Souza, A.J. (2011): Deterministic coastal morphological and sediment transport modeling: A review and discussion. – Reviews of Geophysics 49(2): 1-21.

[2] Cheng, Y., Wang, Y., Jiang, C. (2007): A coupling model of nonlinear wave and sandy seabed dynamic interaction. – China Ocean Engineering 21(1): 77-89.

[3] Díaz, M.C., Fernández-Nieto, E.D., Ferreiro, A.M. (2008): Sediment transport models in shallow water equations and numerical approach by high order finite volume methods. – Computers & Fluids 37(3): 299-316.
[4] Dong, Y., Jiang, J., Liu, X., Wang, D., Zhang, J. (2023): An empirical formula of bottom friction coefficient with a dependence on the current speed for the tidal models. – Frontiers in Marine Science 10: 16p.
[5] Fincham, J.I., Barry, J. (2025): The value of broadscale semi-autonomous seabed monitoring from the perspective of a marine fisheries monitoring programme. – ICES Journal of Marine Science 82(6): 1-6.
[6] Grass, A.J. (1981): Sediment transport by waves and currents. – University College, London, Department of Civil Engineering 52p.
[7] Hou, J., Kang, Y., Hu, C., Tong, Y., Pan, B., Xia, J. (2020): A GPU-based numerical model coupling hydrodynamical and morphological processes. – International Journal of Sediment Research 35(4):
[8] Huai, W., Yang, L., Guo, Y. (2020): Analytical solution of suspended sediment concentration profile: Relevance of dispersive flow term in vegetated channels. – Water Resources Research 56(7): 20p.
[9] Jelti, M., Serghini, A. (2023): Numerical modeling of non-capacity model for sediment transport in open channel hydraulics by Roe scheme with a new discretization of the source term. – Advanced Mathematical Models & Applications 12p.
[10] Jiang, L., Gerkema, T., Idier, D., Slangen, A., Soetaert, K. (2020): Effects of sea-level rise on tides and sediment dynamics in a Dutch tidal bay. – Ocean Science 16(2): 307-321.
[11] Khojasteh, D., Chen, S., Felder, S., Heimhuber, V., Glamore, W. (2021). Estuarine tidal range dynamics under rising sea levels. – PLoS One 16(9): 25p.
[12] Li, S., Tran, H. Q., McCarroll, R. J., Ierodiaconou, D., Babanin, A. V. (2025): Estimation of bottom friction in modelling tidal dynamics of Port Phillip Bay. – Journal of Atmospheric and Oceanic Technology 42(8):1085-1098.
[13] Li, X., Cai, Y., Liu, Z., Mo, X., Zhang, L., Zhang, C., Cui, B., Ren, Z. (2023): Impacts of river discharge, coastal geomorphology, and regional sea level rise on tidal dynamics in Pearl River Estuary. – Frontiers in Marine Science 10: 12p.
[14] Paola, C., Voller, V.R. (2005): A generalized Exner equation for sediment mass balance. – Journal of Geophysical Research: Earth Surface 110(F4): 8p.
[15] Papanicolaou, A., Diplas, P., Dancey, C., Balakrishnan, M. (2001): Surface roughness effects in near-bed turbulence: Implications to sediment entrainment. – Journal of Engineering Mechanics 127(3): 211-218.
[16] Pareta, K. (2024): 1D-2D hydrodynamic and sediment transport modelling using MIKE models. – Discover Water 4(1): 28p.
[17] Penna, N., Coscarella, F., D'Ippolito, A., Gaudio, R. (2020): Bed roughness effects on the turbulence characteristics of flows through emergent rigid vegetation. – Water 12(9): 17p.
[18] Rasyif, T.M., Kato, S., Syamsidik, Okabe, T. (2017): Preliminary study on performance of a coupled hydrodynamic and sediment transport model on small domain. – AIP Conference Proceedings 1892(1): 10p.
[19] Salheddine, M., André, P., Mahmoud, H. (2020): A coupled 1-D/2-D model for simulating river sediment transport and bed evolution. – Journal of Hydroinformatics 22(5): 1122-1137.
[20] Simpson, G., Castelltort, S. (2006): Coupled model of surface water flow, sediment transport and morphological evolution. – Computers & Geosciences 32(10): 1600-1614.
[21] Sun, Z., Li, Y., Wu, N., Fan, Z., Li, K., Sun, Z., Song, X., Xue, L., Jia, Y. (2025): Dynamic Analysis of Subsea Sediment Engineering Properties Based on Long-Term In Situ Observations in the Offshore Area of Qingdao. – Journal of Marine Science and Engineering 13(4): 25p.

[22] Wu, Y., Zhao, E., Li, X., Zhang, S. (2025): Application of wave–current coupled sediment transport models with variable grain properties for coastal morphodynamics: A case study of the Changhua River, Hainan. – Ocean Science 21(1): 473-495.
[23] Yildiz, I., Stanev, E.V., Staneva, J. (2025): Advancing bathymetric reconstruction and forecasting using deep learning. – Ocean Dynamics 75(4): 17p.